Article

Investigation of the Effect of Nanometakaolin on the Compression Behavior of Concrete by Acoustic Emission

Pingping Lu, Zhiqiang Lv,* and Zhen Tan

Cite This: *ACS Omega* 2023, 8, 48915−48924

Read Online

ACCESS | Metrics & More | Article Recommendations

ABSTRACT: To investigate the influence of nanometakaolin (NMK) on the compression behavior of concrete, acoustic emission (AE) is applied to monitor the development of cracks on ordinary concrete as a control sample and concrete with the addition of 1% or 3% NMK during the whole compressive process. The AE parameters (event, count, RA-AF, etc.) and Gaussian Mixture Model (GMM) were analyzed. The results show that the addition of NMK results in a decrease of crack number and crack width. Compared to the control concrete, the concrete with NMK inhibits the initial crack, increases the crack initiation stress and crack damage stress, and improves the energy of crack propagation. Correspondingly, we proposed a critical point where the ringing counts and amplitude fit parameters are less than a certain threshold. This index can be used as a failure precursor for crack instability. According to the criterion and the GMM, what is found from the relation between RA and AF is that the resistance to tensile and shear is improved in the case of the concrete with NMK.
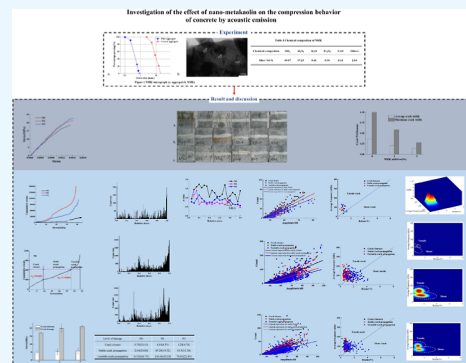
1. INTRODUCTION

Concrete has the advantages of high strength, easy construction, and easy molding. Thus, concrete is widely used in the field of civil engineering.[1] In the service process, it is affected by the harsh environment, such as chloride salt, freeze−thaw cycle, and dry-wet alternating.[2−4] The presence of cracks leads to the corrosion of the concrete structure and the degradation of its mechanical properties. As a result, a vicious cycle makes substantial structures less durable and reduces their useful life. It causes a lot of economic loss. Fully understanding the initiation and propagation of cracks during concrete failure is beneficial for improving the quality of concrete structure, estimating the defects and identifying causes, and ultimately enhancing the durability of concrete.

Therefore, crack initiation and propagation in concrete directly affect its durability. Increasing the energy required for crack initiation and propagation is of great practical significance. Nanometakaolin is a kind of nanoclay with pozzolanic effect, packing effect, and nucleation effect, which has a significant effect on improving durability.[1,2] At present, the effects of NMK on concrete performance mainly focus on improving internal structure, improving macroscopic mechanical properties, and enhancing durability.[3−5] The compression behavior is the most important property of concrete. This behavior includes not only the compressive strength but also the characteristics of crack initiation and propagation. These features are important to the service of concrete. In summary, it is important for NMK to influence concrete performance and concrete compressive behavior. The behavior includes not

only compressive strength but also crack propagation characteristics. However, there are few reports on the effects of NMK on the initiation and propagation of cracks in concrete during compressive failure.

Now, destructive and nondestructive monitoring methods are usually used to study the initiation and propagation of concrete cracks.[5−7] Acoustic emission (AE) is a nondestructive monitoring method with the function of identifying the crack propagation rule and failure mechanism of materials and structures. It is widely used in the field of civil engineering with its advantages of high sensitivity and accurate evaluation.[6−8] The idea of AE was first proposed by Obert in 1941, and it was applied to explore the process of rock failure. In 1959, Rusch introduced AE into the study of the concrete crack propagation process.[9] Crack initiation strength and crack damage are critical to distinguishing between crack initiation and unsteady propagation. Therefore, the AE signal variation characteristics can accurately reflect the crack initiation and propagation law of concrete, the same as the moving point regression method and the stress−strain curve observation method.[10,11] Crack initiation strength and crack damage stress are critical to
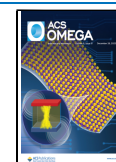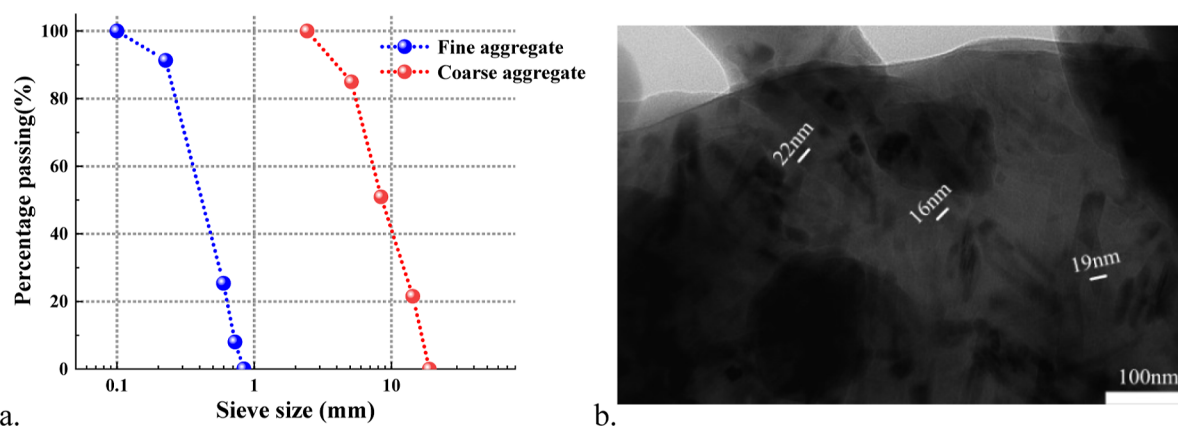
Figure 1. NMK micrograph [(a) Aggregate and (b) NMK].

distinguish between crack initiation and unsteady propagation. Tensile cracks are the dominant crack morphology. A shear crack occurs when the crack grows unsteadily.[12] The AE waveform has a high sensitivity to identify the crack shape, and the tensile crack waveform has the characteristics of a short rise time and high frequency. The rise time of the shear crack waveform is long, and the frequency is low. In summary, AE has achieved remarkable results in identifying crack initiation and propagation in the concrete failure process. However, the AE data are somewhat discrete, which interferes to some extent with the identification of crack propagation properties. Therefore, it is necessary to use statistical features to efficiently identify AE signals.

In the study of the effect of diatomite on the cracking behavior of concrete during the compression process, ordinary concrete and concrete specimens with NMK contents of 1 and 3% (accounting for the mass percentage) were prepared, with 6 pieces in each group, totaling 18 pieces. AE and HD cameras were used to monitor the whole compression process of the three kinds of concrete. The influence of NMK on crack initiation and propagation of concrete was studied according to the changing characteristics of AE parameters (ringing count, amplitude, etc.) during the compression process. Based on the JCMS-III B5706 specification[13] and the Gaussian mixture model (GMM), AE signals were statistically classified to obtain the effect of NMK on the crack morphology of concrete.

2. EXPERIMENT

2.1. Raw Material. Dalian Onoda P·O 42.5R ordinary Portland cement was used in the test. The fine aggregate was river sand, and the coarse aggregate was 5−20 mm gravel. NMK is produced in Lingshou County, Hebei Province, and is calcined at 600−800 C and then milled by a Raymond mill. The microscopic morphology of NMK was observed by a Japanese JEOL JEM-2100 transmission electron microscope. The granulometry distribution of aggregate and NMK is shown in Figure 1. It can be seen that the average layer thickness was about 19 nm. NMK is mainly composed of Si and Al compounds, accounting for 96.3% of the total, as measured by X-ray fluorescence spectrometry, as shown in Table 1.

Table 1. Chemical Composition of NMK

chemical composition	SiO$_2$	Al$_2$O$_3$	K$_2$O	Fe$_2$O$_3$	CaO	others
mass/wt %	49.07	47.23	0.61	0.30	0.16	2.63

2.2. Specimen Preparation. The water-binder ratio of the specimen was 0.45, the water: cementing (cement and NMK): fine aggregate: coarse aggregate was 185:411:613:1190, and the size was 150 mm × 150 mm × 150 mm. In order to study the effect of NMK on the crack propagation process of concrete under compression, ordinary concrete and two kinds of concrete specimens with NMK content (1 and 3%) were prepared in this experiment, and their numbers were recorded as N0, N1, and N3, respectively. The content of diatomite in each group is 6 specimens, for a total of 16 specimens. The production process for the specimen is as follows. (1) NMK was added to water for ultrasonic dispersion for 15 min;[14] (2) The dispersion solution was stirred with the composite material until it was uniform, loaded into the mold for shaking and curing; (3) after 24 h, the mold was removed and placed in saturated calcium hydroxide solution at room temperature (20 ± 2)°C for 28 days.

2..3. Experimental Setup. The velocity of AE signals in each type of concrete has been measured by the pencil-break lead test. The velocities of AE signals in N0, N1, and N2 are 3.28, 3.35, and 3.39 km/s, respectively. Afterward, a WAW-1000D electrohydraulic servo press, a PCI-2 AE test system produced by PAC Company, a HD camera, and a crack width tester were used for the test. The test steps are mainly as follows. (1) The specimen is wiped and polished to meet the requirements of the specification,[15] (2) The sensor type of AE sensors is a ceramic voltage sensor. AE sensors were fixed on both sides of the specimen using vaseline as a coupling agent. (3) In order to avoid the effect of friction, vaseline is applied to the contact point between the specimen and the metallic plate. The specimen is geometrically aligned with the press, and the upper pressing plate is adjusted until it is slightly in contact with the specimen. (4) The AE signal threshold is set to 45 dB, and the gain of the preamplifier and the main amplifier is 40 dB; filter bandwidth 20−400 kHz, sampling frequency 1 MHz; peak identification time 50 μs; impact identification time 300 μs; impact locking time 1000 μs. (5) The loading is controlled by displacement, and the rate is 0.05 mm/min. (6) Lead breaking test is conducted to ensure the regular operation of each instrument. (7) After the end of the compression test, the specimen is taken out to measure the crack width of the noncompression surface by rack width measuring instrument.

3. RESULTS AND DISCUSSION OF TEST RESULTS

3.1. Initiation and Propagation of Crack. The crack generation and development process is an external manifes-

tation of the compression failure of concrete, which is affected by its internal defects and the external stress state. Figure 2
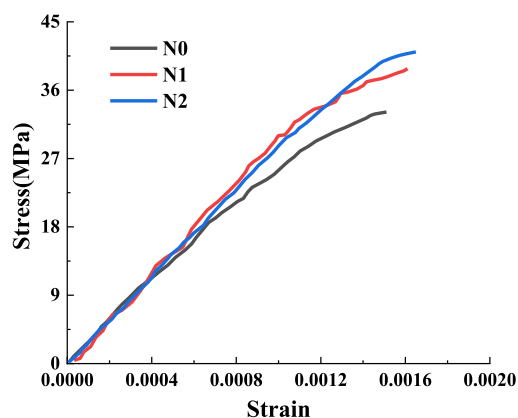

Figure 2. Stress−strain curves.

shows the stress−strain curves for all specimens. At the initial loading stage, the AE signal is stable, and no cracks appear on the specimen surface. With the increase of stress, there is a burst of AE signals, indicating a crack, but no cracking phenomenon is observed on the surface of the specimen. As the stress is further increased, the first visible crack is observed to be generated roughly parallel to the loading direction and is generated at the bottom boundary of the specimen surface. At this time, the loads of N0, N1, and N3 are 15.06, 17.26, and 15.23 MPa, respectively. At this stage, cracks occurred in a stable expansion process under pressure, and the number of AE mutation signals increased significantly. When the stress is about to reach the compressive strength, new cracks are constantly generated, while the cracks on the surface extend and penetrate until the specimen is destroyed, at which stage the AE signal surges. During the failure process, one or two major cracks are detected in N0, while only a small number of surface cracks occur in N1 and N3. The compressive strengths of N0, N1, and N2 are 31.12, 38.83, and 41.04 MPa, respectively. Compared with the stress−strain curves, it can be clearly observed that the elastic moduli of N1 and N2 are

slightly higher than that of N0. In addition, the improvement of the compressive strength of NMK is obvious.

3.2. Fracture Mode. The crack distribution properties of concrete are essential indicators of its durability. Figure 3 shows the surface crack distribution for the three kinds of concrete specimens when the compressive strength is reached. As can be seen from Figure 3, when the compressive strength is reached, 1−2 penetrating cracks occur on the surface of N0, the distribution of small cracks at the edge is relatively dense, and the local damage is apparent. In contrast, the number of surface cracks in N1 and N2 is significantly reduced; some specimens even have no penetrating cracks, and there is basically no local damage at the edge. The number of cracks on N0, N1, and N3 nonstressed surfaces is counted as 51, 28, and 21, respectively. After addition of NMK, the number of cracks on the surface of the specimen is reduced by about 50%, and the higher the dosage, the better the improvement.

To further explore the effect of NMK on crack characteristics, we measured the crack widths and counted them. The maximum crack widths and average crack widths of three kinds of concrete vary with the NMK content, as shown in Figure 4.
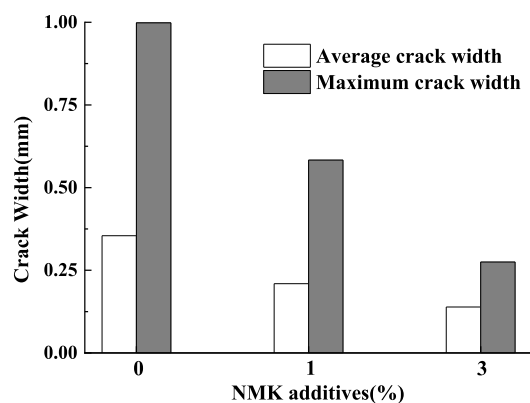

Figure 4. Relation between maximum crack width, average crack width, and NMK additives.

Figure 4 shows that the maximum crack width and average crack width decrease with the increase in NMK content. The
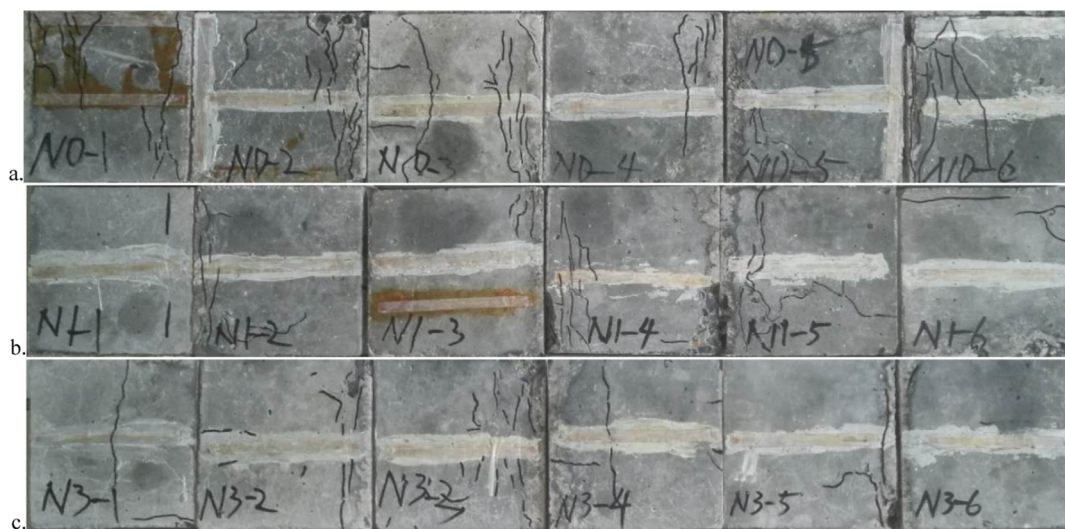

Figure 3. Crack distribution characteristics of the concrete surface (a.N0; b.N1; c.N3).
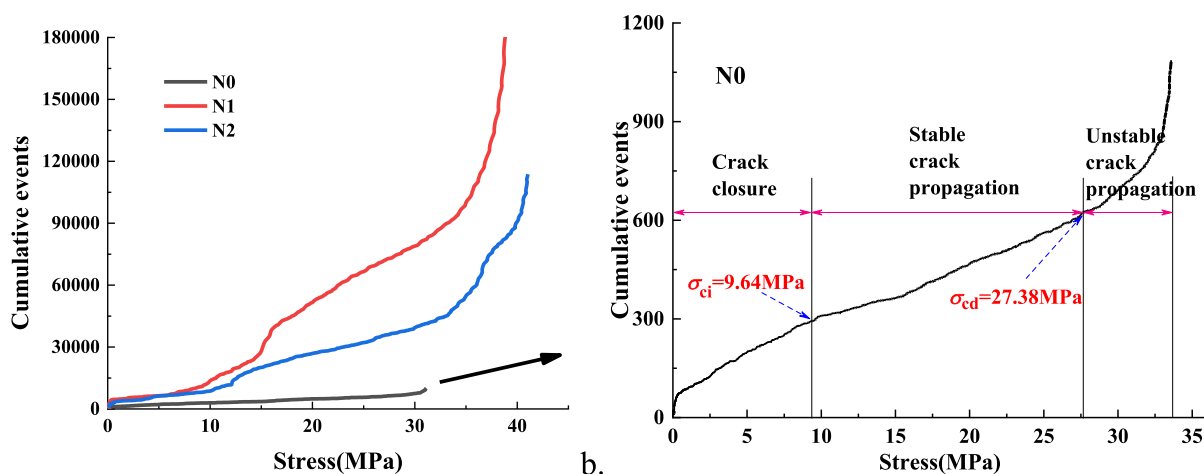
Figure 5. Relation between cumulative events and stress.

maximum crack width and average crack width of N0, N1, and N3 are 0.93 and 0.33, 0.58 and 0.19, and 0.28and 0.13 mm, respectively. Compared with N0, the maximum crack widths of N1 and N3 decreased by 38 and 70%, respectively, and the average crack widths decreased by 42 and 61%, respectively. Therefore, it can be seen in Figure 4 that the NMK content is inversely proportional to the crack width.

3.3. Analysis of the Effect of NMK on the Cracking Process Using the AE Parameters. *3.3.1. Crack Initiation and Crack Damage Identification Using Event.* On the basis of summarizing previous studies, Ranjith obtained the variation characteristics of cumulative events during the onset strength and crack instability strength.[16] The event is defined as a pulse waveform that exceeds a preset threshold voltage and persists for a certain period of time. The event is related to the local failure of concrete during the concrete failure process. In the following, N0 is used as an example to identify the onset strength and crack instability strength through cumulative events. The variation of cumulative events with stress is shown in Figure 5a–b. As can be seen from Figure 5b, crack growth during the loading process of the specimen can be divided into three stages: crack closure, stable crack propagation, and unstable crack propagation.[8] In the crack closure stage, the cumulative events are mainly caused by crystalline friction and microcrack closure in concrete and are relatively small in number. When the stress reaches the crack initiation stress, the crack expands steadily, and the cumulative number of events increases linearly. The stress increases and enters the stable expansion stage; the crack expands steadily, and the cumulative events increase linearly. When the stress reaches the crack damage stress, cracks gather, macro failure occurs, considerable energy is released, and the cumulative events deviate from the linear stage. The stress is further increased to the stage of unstable expansion, where the crack grows unsteadily and the cumulative number of events increases approximately exponentially.

The dependence of the initiation strength on the crack instability strength as a function of the NMK content is obtained from the law of variation of cumulative events with stress during three types of concrete compression failures, as shown in Figure 6. It can be seen from Figure 6 that the crack initiation strength and crack instability strength of concrete specimens increase with increase in NMK content. The crack initiation stresses for N0, N1, and N3 were 7.21, 8.40, and 9.10
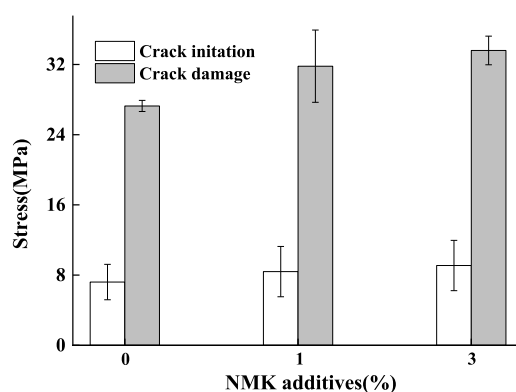

Figure 6. Relation between crack initiation, crack damage, and NMK additives.

MPa, respectively, and the crack damage stresses were 27.28, 31.81, and 33.60 MPa. The crack initiation stress and crack damage stress of N1 and N3 are increased by 17, 26 and 17, 23%, respectively, compared with N0. The results show that the crack initiation strength and crack instability strength increase with the increase of NMK content. Previous research results showed that NMK participated in the hydration process to generate hydrated calcium silicate gel (C−S−H). Literature[3] confirmed from both micro and macro aspects that C−S−H effectively improved the mechanical properties of mortar−aggregate interface (ITZ) and thus improved the yield strength of concrete and the elastic modulus. Therefore, NMK can improve the compressive strength of concrete.

3.3.2. Crack Growth Analysis Using Count Rate. The count rate is the primary parameter of the AE signal, which is used to investigate the crack propagation properties of the concrete failure process. The count change properties of the three types of concrete during the loading process are shown in Figure 7. As can be seen from Figure 7, when the stress is less than 0.8 relative stress, the count rate changes relatively calmly, and its "active period"[17] is mainly concentrated in the stage of unstable crack growth. It can be seen in Figure 7a that the count rate of N0 in the crack compaction stage, the stable expansion stage, and the initial stage of the unstable expansion stage is the same, below 100. It is not until the compression intensity is about to be reached that the count rate increases significantly and the peak count rate goes to 300. Figure 7 shows that when the relative stress of N1 and N3 is less than
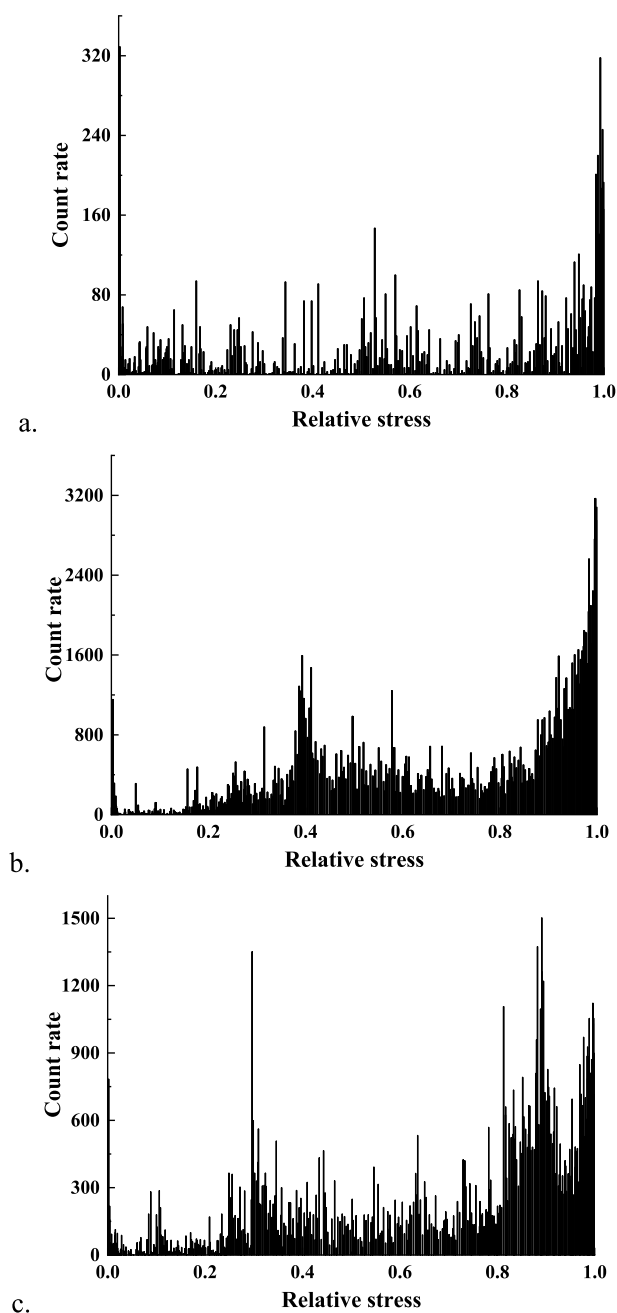
Figure 7. Relation between count rate, cumulative counts, and NMK additives [(a) N0; (b) N1; (c)N3].

0.3, the count rate is relatively calm, below 400. At the stage of 0.3−0.8, the peak count rate increases significantly, which is 150 and 600, respectively. For relative stresses greater than 0.8, the peak count rates reach about 3200 and 1500, respectively. The test results showed that the change in count rate reflected the crack development of concrete.

When the relative stress is less than 0.3, the peak count rates of N1 and N3 are significantly lower than those of N0, indicating that the addition of NMK improves the internal structure and inhibits the occurrence of microcracks. In the range 0.3−0.8, the crack grows steadily, the count rate fluctuates within a specific range, the peak value increases significantly, and the stress is redistributed to a certain extent. When the relative stress is 0.8−1, the count rate of N0 surges when the compressive strength is about to be reached, and the

distribution of the "active period" is relatively concentrated, indicating that the stress concentration phenomenon is evident. While the distribution range of the "active period" of N1 and N3 is all over the whole unstable expansion stage, even two "active periods" appear. After the energy is released once, the count drops sharply, and the stress is redistributed. This phenomenon suggests that an increase in the NMK content increases the ductility during failure.

To further investigate the variation rule of the count rate, the mean and standard deviation of the count rate are used to reflect the influence of NMK on the crack growth law in the concrete failure process. The mean values and standard deviation of the count rate for the three types of concrete crack growth stages are listed in Table 2. As seen from Table 2,

Table 2. Mean and Variance of Count Rate in Crack Propagation Stage[a]

level of damage	N0	N1	N3
crack closure	0.76(24.41)	4.04(6.53)	3.28(4.78)
stable crack propagation	2.04(24.84)	45.29(19.52)	19.5(11.38)
unstable crack propagation	63.50(68.75)	156.00(35.23)	70.93(22.45)

[a]Note: Coefficients of variation is given in parentheses.

both the mean and variance of the count rate showed an increasing trend with the increase of scale in the process of crack propagation. The research in the literature[18] shows that the occurrence of local cracks is the root cause of irregular count rate. In the first stage (crack closure stage), the mean value of the count rate of N1 and N3 is small and the count rate changes are stable, while the variance of the count rate of N0 is large due to more internal defects. The stress reaches the cracking intensity and further increases into the second stage (stable expansion stage); count rate stability weakens, and the mean and variance increase obviously. The stress reaches the instability expansion strength and enters the third stage (unstable expansion stage). As the crack continues to expand, it undergoes an unstable expansion, resulting in a sudden increase in the count rate and increased volatility. Due to the large number of pores and cracks in N0, the phenomenon of stress concentration easily occurs, so the mean and variance of the third-order count rate surge, while N1 and N3 steadily increase during the process of crack propagation, indicating that the internal structure of NMK concrete is relatively dense. The stability of crack propagation during compression is enhanced.

3.3.3. Crack Multiscale Analysis Using b Value. The distribution characteristics of AE event frequency and amplitude are similar to those of an earthquake. After some modification, the relationship between AE event frequency and amplitude is obtained, as shown in eq 1.[8]

$$\log_{10} N = a - b(A/20) \tag{1}$$

where A is the amplitude of AE events, N is the cumulative number of AE events larger than A, and a and b are the fitting coefficients related to the crack scale. When a microscopic crack occurs, the amplitude of the released AE signal is small and the b value is large, whereas if the b value is small, it can accurately reflect the crack propagation law during the failure process of materials or structures. According to formula 1, the

b value in the three kinds of concrete is calculated, and the results are shown in Figure 8.
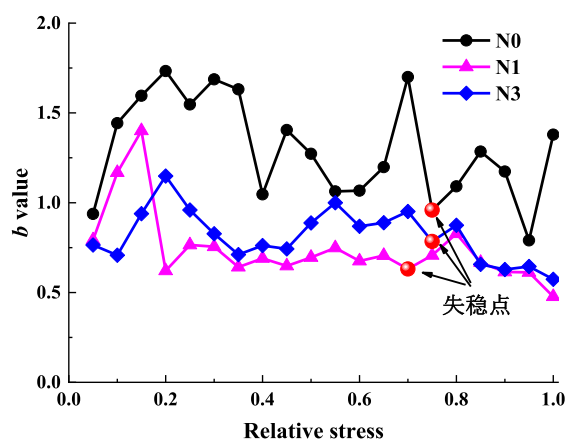

Figure 8. Relation between the *b* value and relative stress.

The calculated *b* value is usually divided into three types: stress level, number of AEs, and crack propagation stage.[9−11] For the comparative analysis, the value of *b* in this section is the level of relative stress increase per 0.1. As can be seen from Figure 8, the *b* value exhibits a rising, fluctuating, and continuously decreasing variation law in the three types of concrete compression processes, but the magnitude of the *b* value and the range of the fluctuations are significantly different. Under the action of low stress, microcracks occur in the specimen, and the *b* value of the low amplitude released shows an increasing trend. When the stress reaches the crack initiation strength, the crack occurs, the AE amplitude increases, and the *b* value decreases. The stress continues to increase; the crack expands steadily; the AE signal is stable; and the *b* value fluctuates within a certain range. When the stress reaches the crack instability strength, the macro instability crack occurs, the release energy is large, the number of high-amplitude signals increases, and the *b* value decreases to the minimum value. During the continuous increase of stress to compressive strength, unstable expansion occurs rapidly after the emergence of new cracks, so the *b* value rises first and then continues to decline.

When the relative stress is less than 0.3, the increase of *b* value of the three types of concrete is N0 > N1 > N3, indicating that the higher the NMK content, the more pronounced the inhibition effect on the internal microcrack. When the relative stress ranges from 0.3 to 0.8, the *b* value fluctuates within a specific range; N0 has the highest volatility, N3 is second, and N1 is the least. For the stress around 0.8, the *b* value obtained by the three types of concrete reaches a minimum value, which is related to the high-amplitude signal released during crack propagation. It can be used as the basis for judging macro instability, which is consistent with previous research results.[20] The stress further increases to failure, and the *b* value of the three types of concrete shows a downward trend. In the process of crack initiation and propagation, therefore, it can be concluded that the addition of NMK can increase the stability of crack propagation and improve the brittle properties of the concrete, which is consistent with the aforementioned change in the count rate properties.

3.3.4. Crack Growth Analysis Count and Amplitude. The law of crack growth in concrete compression failure presents

apparent stages. The variation characteristics of the count and amplitude of the crack growth stage of the specimen are listed in Figure 9. As can be seen in Figure 9, the range of counts and
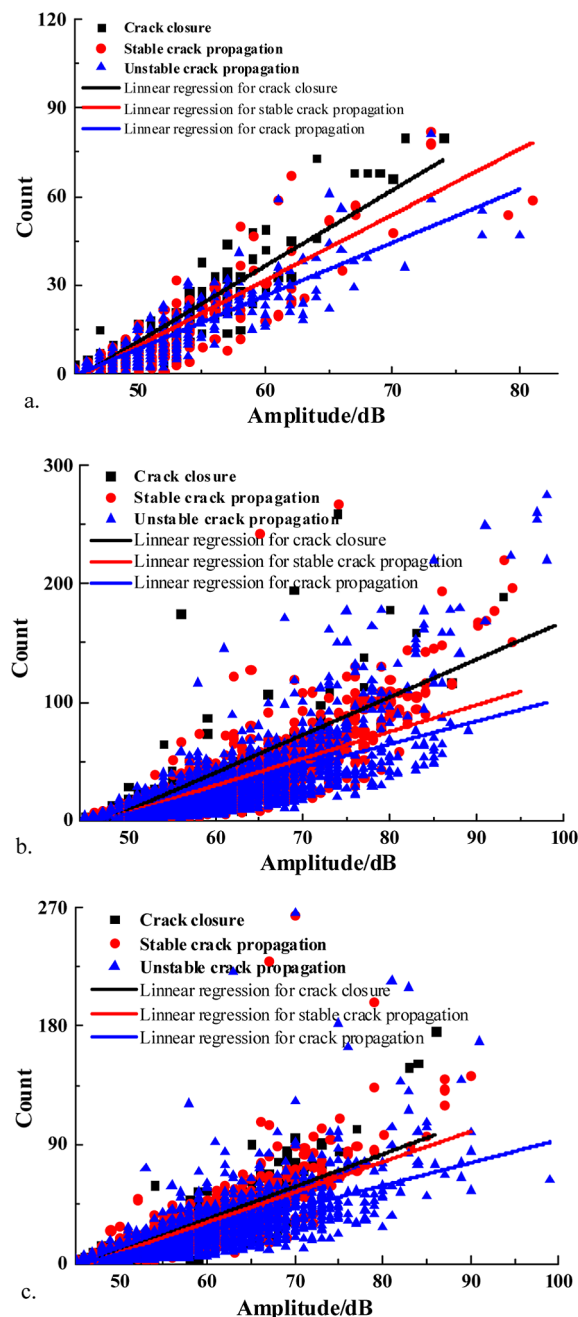

Figure 9. Relation between the count and amplitude [(a) N0; (b) N1; (c) N3].

amplitudes changes significantly as the cracks continue to expand during the failure of the specimen. Figure 9a shows that the amplitude of the N0 crack is distributed in the range of 45−70 dB before the nonstable propagation, which is consistent with previous research results.[21] In the stage of unstable expansion, the amplitude distribution range increases between 45 and 85 dB. As shown in Figure 9b,c, before the crack propagation of N0 and N1 is unstable, the amplitude is distributed in the range of 45−85 dB (due to the dispersion of data in N1, very few signal amplitudes are greater than 85

dB).[19,22] In the stage of unstable expansion, the amplitude is distributed between 45 and 100 dB. During the compression process, N0 counts are distributed in 0−100, and N1 and N3 are distributed in 0−280, which is more than twice as many as N0. The experimental results show a clear increase in the AE signal amplitude and the range of the count distribution when NMK is added, which proves that the energy required for the crack propagation process of NMK concrete increases.

To further distinguish the variability characteristics of the counts and amplitudes during crack growth, a linear fit was performed to the relationship between the counts and amplitudes at different crack growth stages. The results are listed in Table 3. However, there are some differences in the

Table 3. Count and Amplitude Fitting Parameter of Crack Propagation Stage[a]

damage stage	N0		N1		N3	
	a	|c|	A	|c|	a	|c|
crack closure	2.56	117.32	3.19	150.72	2.47	114.71
stable crack propagation	2.22	101.67	2.26	106.12	2.30	106.84
unstable crack propagation	1.80	81.60	1.94	90.80	1.73	79.83

[a]Note: a-value is slope, c-value intercept.

amplitude and count distribution ranges of the three types of concrete during the compression process; the variation trend is consistent. The fitted values of a and |c| are larger than 2 and 100, respectively, before the growth of the unstable crack and smaller than 2 and 100, respectively, during the growth of the unstable crack. It is shown that the count and amplitude fitting parameters can be used as a basis for predicting the failure of the instability when it is less than a particular threshold value.

3.3.5. Crack Mode Analysis Using RA-AF. Ohtsu used RA and average frequency (AF) parameters to identify the crack morphology according to the difference in AE waveform released by different crack morphologies.[7] RILEM specification RA is the rise time divided by the peak waveform voltage. The unit is us/V or ms/V. AF is the count divided by the duration, expressed in kHz.[12] In this paper, the norm method[13] is adopted to classify the crack morphology according to the RA and AF distribution characteristics. Figure 10 shows the distribution features of RA and AF in the crack propagation process for the three types of concrete. As can be seen from Figure 10, the range of variation of RA increases and the range of variation of AF decreases during the propagation of the concrete crack, indicating that the crack morphology gradually changes from tensile to shear. Before the crack propagation, the AF of N0 is less than 150 kHz, the distribution range of N1 and N3 is less than 200 kHz, and the distribution range of the RA value is roughly equal. According to the AE signal, the three types of concrete are mainly characterized by tensile cracks, and basically, no shear cracks occur. In the unstable expansion stage, the RA value increases significantly, and the AF value shows a downward trend. In this stage, the N0 signal RA is less than 2 ms/V, and the maximum RA value of the N1 and N3 signals reaches 4 ms/V.

Before the unstable expansion, the released AF values of N1 and N3 were larger than those of N0, indicating that the tensile strength of the NMK concrete was enhanced. In the unstable expansion stage, the RA value of the AE signal generated by N1 and N3 is more than twice that of N0, which indicates that
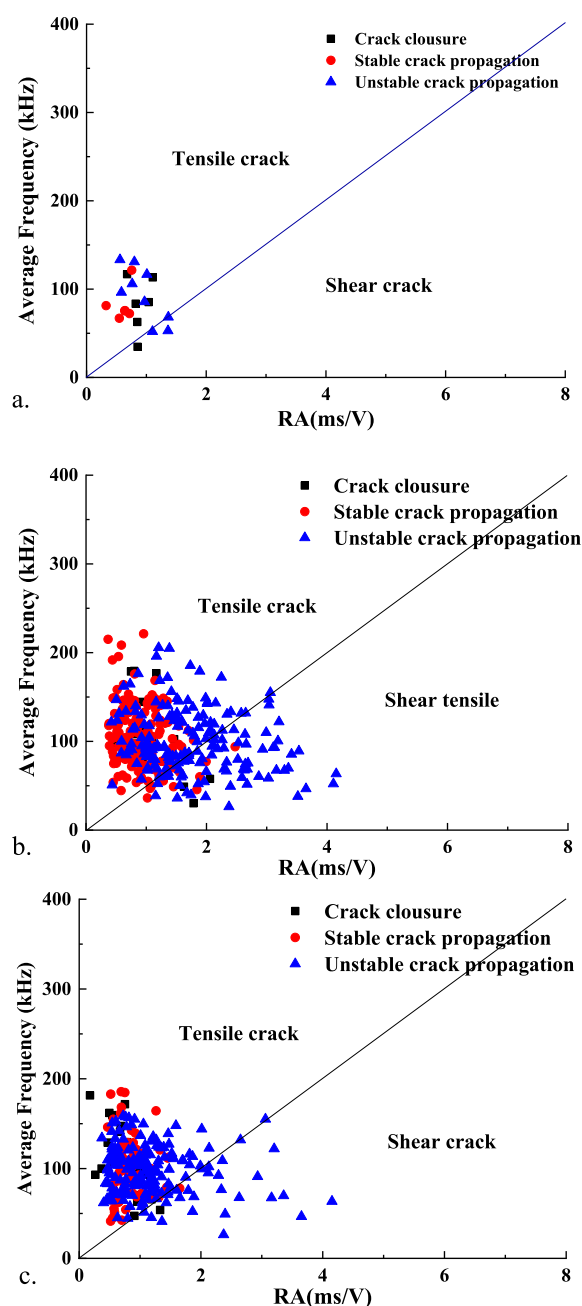

Figure 10. AF and RA distribution characteristics [(a) N0; (b) N1; (c) N3].

NMK improves the antishear performance to some extent. Therefore, the experimental results show that NMK can improve the tensile and shear strength of concrete during the crack propagation process.

3.3.6. Crack Mode Analysis Using GMM Model. The GMM model is applied to classify AE signals; it is necessary to use EM algorithm to estimate GMM parameters, and these parameters need to be transformed under the Bayes idea.

The expression of GMM model is shown in eq 2[23]

$$p(x) = \sum_{k=1}^{K} \pi_k N(x|\mu_k, \Sigma_k)$$

(2)

where $p(x)$ is the probability density function, which follows the normal or Gaussian distribution. x is a two-dimensional
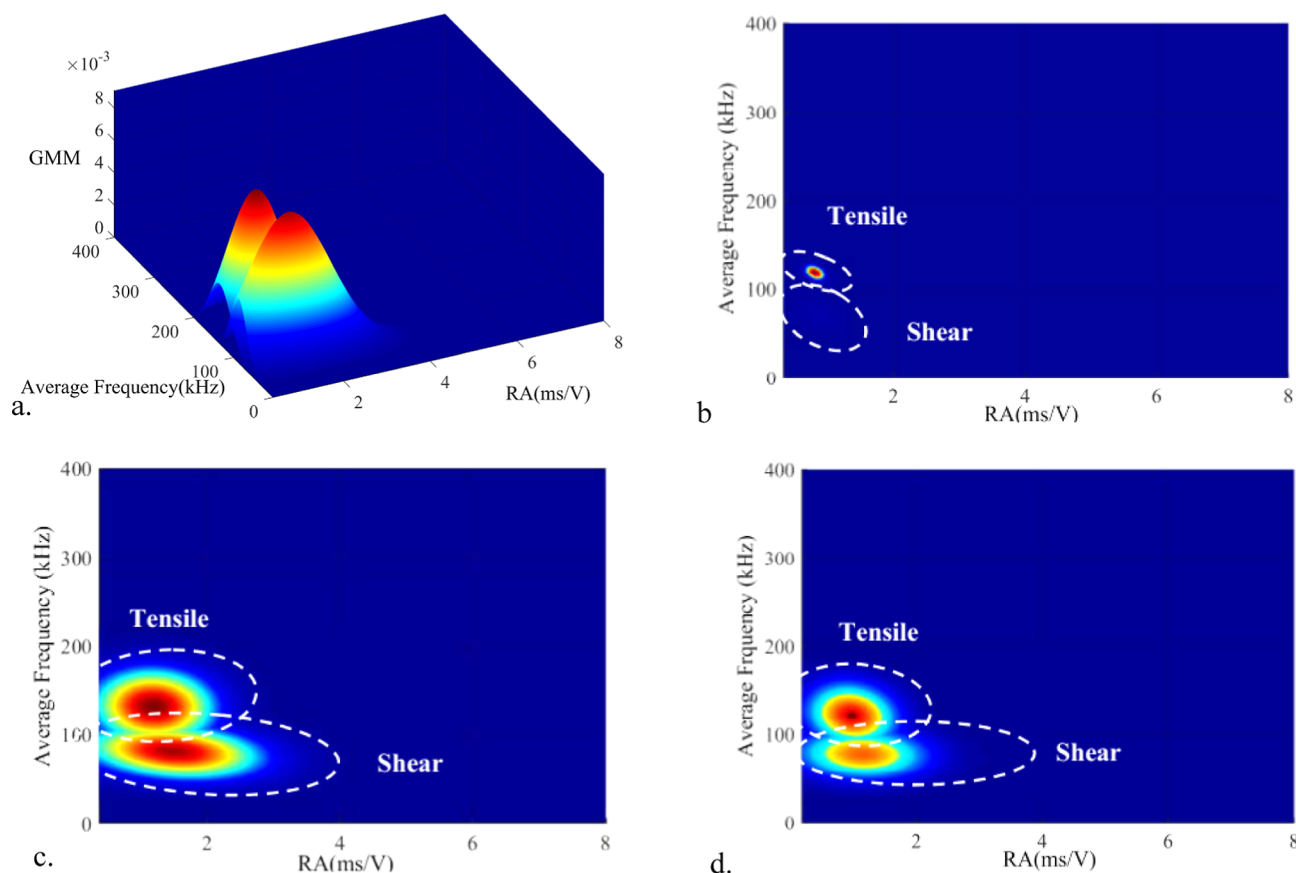
Figure 11. Crack classification based on GMM. [(a) N1 crack distribution sensitivity; (b) N0 crack classification; (c) N1 crack classification; (d) N3 crack classification].

plane coordinate, representing a two-dimensional vector. π_k is the weight coefficient, $\sum_{k=1}^{K} \pi_k = 1$, $0 \leq \pi_k \leq 1$, $N(x|\mu_k,\Sigma_k)$ is the KTH component of the mixed model, and two-dimensional Gaussian distribution is adopted in this paper, so $k = 2$ is taken.

When solving GMM, three parameters in the EM algorithm model need to be estimated, namely π, μ, and Σ, so formula 2 is rewritten in the following form[24]

$$p(x|\pi, \mu, \sum) = \sum_{k=1}^{K} \pi_k N(x|\mu_k, \Sigma_k) \qquad (3)$$

In order to find π, μ, and Σ, it is necessary to estimate the maximum likelihood function of these three parameters in eq 3 until the algorithm converges.

MATLAB compiled the GMM program to analyze the values of RA and AF, and the results are shown in Figure 11. As can be seen in Figure 11, the distribution of tensile and shear cracks and the influence of NMK can be more intuitively identified after the GMM classification of the AE signals of the three types of concrete. In Figure 11, an excessive shift from red to blue represents a gradual decrease in probability density. This representation removes the overlap and coverage caused by the excessive data volume in the graph drawing process and clearly displays the signal density in the form of a probability density.

According to the calculation results, the distribution of three kinds of shear and tensile cracks in concrete is drawn with white dotted lines (Figure 11b−d). According to the change of probability density and classification region, it can be clearly

seen that GMM can effectively distinguish between tensile crack and shear crack and identify RA and AF distribution ranges. The RA and AF values of the released AE signals for N1 and N0 are significantly higher than those for N0. At the same time, the color change of the probability density distribution shows a significant increase in the fraction of shear cracks with NMK added, which also indicates that the tensile and shear resistance of the concrete are improved.

4. IMPLICATIONS

The effect of diatomite on the compressive behavior (crack width, crack propagation, cracking scale, and crack mode) of concrete has been investigated by AE. The results demonstrate that diatomite can increase the crack initiation stress, which is the critical value of the transformation from micro crack to macro crack. The enhancement of the crack initiation stress has important implications for some crucial structures that are sensitive to cracks. Nuclear engineering, for example, is sensitive to macroscopic cracks.[25−27] For fundamental infrastructure, crack damage stress is a more important indicator, representing the transition from stable cracks to instability. Therefore, diatomite has practical significance for improving the crack damage stress of concrete. In addition, the increase of compressive strength directly affects the design and stability of the concrete structure.

From the analysis of the above results, AE can clearly reveal the compression behavior of concrete. The cumulative events, ringing count rates, and statistical characteristics were analyzed to identify the stages of crack propagation (crack closure, stable crack propagation, and unstable crack propagation). In

addition, *b* value can reflect the multiscale cracks of concrete. The identification of minimum b value is conducive to providing early warning information.[28] However, the minimum *b* value is different for concrete containing diatomaceous earth, which is not conducive to providing early warning information.[29] It is interesting that the fitting values of amplitude and count less than 2 as early warning information are feasible for all specimens. This finding provides a feasible method for damage warning of concrete failure for different concretes. Next, the application of the Gaussian mixture model on the basis of RA and AF to identify crack morphology is advantageous compared with the RILEM.[30] Finally, a number of important limitations need to be considered. Sensor spacing should be considered due to attenuation of the signal in the actual structure. Noise filtering is another important issue. Compared with the laboratory, noise interference is complicated in practical engineering. Therefore, it is of practical significance to remove noise according to practical application.

5. CONCLUSIONS

To explore the effect of NMK on the compression process of concrete, the AE method was used to monitor the uniaxial compression process of ordinary concrete and concrete with two NMK mixtures. The AE signal was analyzed to explore the effect of high territory on the compression behavior of concrete. The main conclusions are as follows.

The addition of NMK increases the amount and strength of cracks in the concrete. The number of cracks, average crack width, and maximum crack width were reduced by about 50, 40, and 60%, respectively, for NMK levels of 1 and 3%. The crack initiation stress and crack damage stress are increased by 17, 26, 17 and 23%, respectively. The enhancement of crack initiation stress and damage stress is of great significance to improve the service life of concrete.

The variation of the AE parameters during the compression process indicates that the addition of NMK has a significant impact on crack development in concrete. NMK inhibits crack generation at the initial stage of loading and increases the energy required for crack propagation. At the same time, the obtained count and amplitude fit parameters can be used as precursor information to predict macroscopic instabilities when they are below a certain threshold. This finding provides a novel approach to concrete damage warnings.

The AE signal of NMK concrete in the process of compression failure is identified based on the norm method and GMM. The distribution of AF and RA values for N1 and N3 is significantly larger than that for N0, suggesting that NMK improves the tensile and shear capacity of the concrete.

■ AUTHOR INFORMATION

Corresponding Author

Zhiqiang Lv − *School of Civil Engineering, Liaoning Technical University, Fuxin, Liaoning 123000, China*; Email: lv18342241772@163.com

Authors

Pingping Lu − *School of Civil Engineering, Liaoning Technical University, Fuxin, Liaoning 123000, China*; orcid.org/0009-0003-9258-2991

Zhen Tan − *Liaoning Non-ferrous Geological Exploration and Research Institute Co., Ltd., Shenyang, Liaoning 110013, China*

■ REFERENCES

(1) Xie, C.; Yuan, L.; Zhao, M.; Jia, Y. Study on failure mechanism of porous concrete based on acoustic emission and discrete element method. *Constr. Build. Mater.* **2020**, *235*, 117409.

(2) Suzuki, T.; Ohtsu, M. Damage estimation of concrete canal due to earthquake effects by acoustic emission method. *Constr. Build. Mater.* **2014**, *67*, 186−191.

(3) Geng, J.; Sun, Q.; Zhang, W.; Lü, C. Effect of high temperature on mechanical and acoustic emission properties of calcareous-aggregate concrete. *Appl. Therm. Eng.* **2016**, *106*, 1200−1208.

(4) Geng, J.; Sun, Q.; Zhang, Y.; Cao, L.; Zhang, W. Studying the dynamic damage failure of concrete based on acoustic emission. *Constr. Build. Mater.* **2017**, *149*, 9−16.

(5) Ramezanianpour, A. A.; Bahrami Jovein, H. Influence of metakaolin as supplementary cementing material on strength and durability of concretes. *Constr. Build. Mater.* **2012**, *30*, 470−479.

(6) Morsy, M. S.; Shoukry, H.; Mokhtar, M. M.; Ali, A. M.; El-Khodary, S. A. Facile production of nano-scale metakaolin: An investigation into its effect on compressive strength, pore structure and microstructural characteristics of mortar. *Constr. Build. Mater.* **2018**, *172*, 243−250.

(7) Qian, X. Q.; Li, Z. J. The relationships between stress and strain for high-performance concrete with metakaolin. *Cem. Concr. Res.* **2001**, *31*, 1607−1611.

(8) Siddique, R.; Klaus, J. Influence of metakaolin on the properties of mortar and concrete: A review. *Appl. Clay Sci.* **2009**, *43*, 392−400.

(9) Abed, M. K.; Habeeb, Z. D. Mechanical behavior of self-compacting concrete containing nano-metakaolin. *Eng. Sci.* **2017**, *5* (25), 1750−1758.

(10) Wu, J.; Wang, E.; Ren, X.; Zhang, M. Size Effect of Concrete Specimens on the Acoustic Emission Characteristics under Uniaxial Compression Conditions. *Adv. Mater. Sci. Eng.* **2017**, *2017*, 1−12.

(11) Gu, Q.; Ma, Q.; Jia, Z.; Tan, Y.; Zhao, Z.; Huang, D. Acoustic emission characteristics and damage model of cement mortar under uniaxial compression. *Constr. Build. Mater.* **2019**, *213*, 377−385.

(12) Haneef, T. K.; Kumari, K.; Mukhopadhyay, C. K.; Venkatachalapathy; Rao, B. P.; Jayakumar, T. Influence of fly ash and curing on cracking behavior of concrete by acoustic emission technique. *Constr. Build. Mater.* **2013**, *44*, 342−350.

(13) Ohtsu, M. Prospective applications of AE measurements to infra-dock of concrete structures. *Constr. Build. Mater.* **2018**, *158*, 1134−1142.

(14) Noorsuhada, M. N. An overview on fatigue damage assessment of reinforced concrete structures with the aid of acoustic emission technique. *Constr. Build. Mater.* **2016**, *112*, 424−439.

(15) Behnia, A.; Chai, H. K.; Shiotani, T. Advanced structural health monitoring of concrete structures with the aid of acoustic emission. *Constr. Build. Mater.* **2014**, *65*, 282−302.

(16) Hu, S.; Lu, J.; Fan, X. Summary of experimental study on fracture properties of concrete. *ASCE J. Hydraul. Div.* **2014**, *S1*, 10−18.

(17) Zhou, H.; Meng, F.; Lu, J.; Zhang, C. Q.; Yang, F. J. Discussion on methods for calculating crack initiation strength and crack damage strength for hard rock. *Rock Soil Mech.* **2014**, *35* (4), 913−918.

(18) Ranjith, P. G.; Jasinge, D.; Song, J. Y.; Choi, S. K. A study of the effect of displacement rate and moisture content on the mechanical

properties of concrete: Use of acoustic emission. *Mech. Mater.* **2008**, *40*, 453−469.

(19) Recommendation of RILEM TC 212-ACD: acoustic emission and related NDE techniques for crack detection and damage evaluation in concrete.

(20) JCMS-III B5706. Monitoring method for active cracks in concrete by acoustic emission.

(21) Fan, Y.; Zhang, S.; Kawashima, S.; Shah, S. P. Influence of kaolinite clay on the chloride diffusion property of cement-based materials. *Cem. Concr. Compos.* **2014**, *45*, 117.

(22) GB/T50081−2002, Standard test method for mechanical properties of ordinary concrete.

(23) Guo, Q.; Xi, B.; Li, Z.; Zheng, X.; Tian, J.; Zhu, H. Experimental research on relationship between frequency characteristics of acoustic emission and strength parameter in concrete. *J. Cent. South Univ.* **2015**, *46* (4), 1482−1488.

(24) Wei, H.; Liu, Y.; Li, J.; Wang, F.; Zheng, J.; Yuan, Z. Characterizing fatigue damage evolution in asphalt mixtures using acoustic emission and Gaussian mixture model analysis. *Constr. Build. Mater.* **2023**, *409*, 133973.

(25) Li, Z.; Shah, S. P. Microcracking in concrete under uniaxial tension. *ACI Mater. J.* **1994**, *91* (4), 372−381.

(26) Ma, G.; Li, H. Acoustic emission monitoring and damage assessment of FRP-strengthened reinforced concrete columns under cyclic loading. *Constr. Build. Mater.* **2017**, *144*, 86−98.

(27) Sagar, R. V.; Prasad, B. R.; Kumar, S. S. An experimental study on cracking evolution in concrete and cement mortar by the b-value analysis of acoustic emission technique. *Cem. Concr. Res.* **2012**, *42*, 1094−1104.

(28) Yun, H. D.; Choi, W. C.; Seo, S. Y. Acoustic emission activities and damage evaluation of reinforced concrete beams strengthened with CFRP sheets. *NDT&E Int.* **2010**, *43*, 615−628.

(29) Prem, P. R.; Murthy, A. R. Acoustic emission monitoring of reinforced concrete beams subjected to four-point-bending. *Appl. Acoust.* **2017**, *117*, 28−38.

(30) Li, H. *Statistical learning method*; Tsinghua University Press: Beijing, 2011, pp 155−166.